MOLECULAR AND CELLULAR BIOLOGY, May 1993, p. 2929–2941
0270-7306/93/052929-13$02.00/0

Vol. 13, No. 5

Mouse β-Globin DNA-Binding Protein B1 Is Identical to a Proto-Oncogene, the Transcription Factor *Spi-1*/PU.1, and Is Restricted in Expression to Hematopoietic Cells and the Testis

DEBORAH L. GALSON,[1]†* JACK O. HENSOLD,[2] TERRY R. BISHOP,[3] MARTIN SCHALLING,[1] ALAN D. D'ANDREA,[4] CAROL JONES,[5] PHILIP E. AURON,[6] AND DAVID E. HOUSMAN[1]

Center for Cancer Research and Department of Biology, Massachusetts Institute of Technology, Cambridge, Massachusetts 02139[1]; University/Ireland Cancer Center and Department of Medicine, Case Western Reserve University Medical School, Cleveland, Ohio 44106[2]; Division of Hematology, Department of Pediatrics, Johns Hopkins University School of Medicine, Baltimore, Maryland 21205[3]; Division of Pediatric Oncology, Dana-Farber Cancer Institute,[4] and Center for Blood Research and Department of Pathology,[6] Harvard Medical School, Boston, Massachusetts 02115; and Department of Biochemistry, Eleanor Roosevelt Institute for Cancer Research and University of Colorado Health Sciences Center, Denver, Colorado 80262[5]

Received 10 August 1992/Returned for modification 15 September 1992/Accepted 4 February 1993

The hematopoietic-specific DNA-binding protein B1 binds to the DNA consensus sequence AAAGRGGAARYG located twice in intervening sequence 2 of both of the mouse β-globin genes (D. L. Galson and D. E. Housman, Mol. Cell. Biol. 8:381–392, 1988). B1 was cloned by expression of a murine erythroleukemia (MEL) cell cDNA library in transfected COS cells and screening by electrophoretic mobility shift analysis. B1 is identical to the proto-oncogene *Spi-1*/PU.1 (*Spi-1*), an *ets* family member. Protein-DNA contacts are shown to resemble those of the helix-turn-helix homeodomain proteins. By Northern (RNA) analysis, we found that *Spi-1* mRNA is present at low levels during murine CFU-E maturation and is at least 20-fold higher in uninduced MEL, a transformed proerythroblast-like cell line which contains an activating/transforming insertion of spleen focus-forming virus at the *Spi-1* locus. Dimethyl sulfoxide-induced MEL cell differentiation decreases *Spi-1* mRNA to approximately 20% of the uninduced level before commitment occurs. In addition to erythroid cells, *Spi-1* mRNA is present in B cells, myelomonocytes, and mast cells but not in T cells and nonhematopoietic cell types. In situ hybridization demonstrated *Spi-1* mRNA expression in bone marrow, spleen, interstitial nonhepatocytes of the liver, and interstitial nontubular cells of the testis. The *Spi-1* locus was mapped on human chromosome 11 to the same interval as ACP2 (lysosomal acid phosphatase), between the anonymous DNA markers D11S33 and D11S14. This region has not yet been found to be associated with a human malignancy.

We have previously identified by electrophoretic mobility shift analysis (EMSA) several factors in murine erythroleukemia (MEL) cells that bind to specific sequences within the mouse β-major (β^M)-globin intervening sequence 2 (IVS2) (27). The region encompassing these sites has been observed by others to be a tissue-specific DNase I-hypersensitive site and the border of nucleosome phasing on the globin gene in erythroid cells (7, 39, 78). This region includes two homologous sites for factor B1 (B1-A and B1-B) and one site each for factors Oct-1 (40) and B2 (now designated GATA-1 [61]). Only the regions of the IVS2 containing these binding sites are homologous between the β^M- and β-minor (β^m)-globin genes, further suggesting a functional importance for these interactions. The factor B1 core consensus binding site, AAAGRGGAARYG, was derived from the four B1 sites in the β-globin genes, and EMSA showed that factor B1 was present in erythroid cells (except CB5 cells, a BFU-E-like cell line), B cells, and myelomonocytes but not in T cells or in the many nonhematopoietic cell types assayed (27).

* Corresponding author. Electronic mail address: Galson@Calvin.BWH.Harvard.Edu.

† Present address: Division of Hematology-Oncology, Department of Medicine, Brigham & Women's Hospital, Harvard Medical School, Boston, MA 02115.

We report here the cloning of the cDNA for MEL factor B1 by using a modification of the approach taken by Tsai et al. (83), involving a mammalian expression system combined with EMSA analysis of extracts from the transfected COS cells as the detection method. The cDNA sequence revealed that factor B1 is identical to the proto-oncogene/DNA-binding factor *Spi-1*/Pu.1/*Sfpi-1* (*Spi-1* stands for spleen focus-forming virus [SFFV] proviral integration 1) (33, 47, 55, 65), an *ets* gene family member which had been previously cloned by different methodologies. On the basis of analysis of the protein sequence and protein-DNA contacts, we propose that there are structural similarities between the DNA-protein interactions of the ETS domain, in particular that of *Spi-1*, and of the helix-turn-helix (HTH) motif of homeodomain proteins.

MEL cells are generated by transformation with the Friend virus which is a complex of a replication-defective SFFV and a replication-competent Friend murine leukemia virus (F-MuLV) helper (for a review, see reference 43) and are thought to be blocked from further differentiation at the proerythroblast stage (for a review, see reference 53). Moreau-Gachelin et al. (56) have shown that in at least 95% of MEL cell lines, SFFV has integrated several kilobases upstream of the *Spi-1* gene in the opposite orientation to the transcription unit. As a result of this integration event, *Spi-1*

mRNA expression is elevated and is believed to play a role in the block to differentiation associated with transformation (3, 54). MEL cells can be induced by dimethyl sulfoxide (DMSO) and various other chemical agents to undergo a differentiation program which morphologically and biochemically resembles that of normal murine erythropoiesis (53, 85). Hence, we have examined the expression of *Spi-1* mRNA in normal erythroid differentiation and during DMSO-induced MEL cell differentiation. Controversy exists in the literature regarding the tissue specificity of *Spi-1* mRNA expression (47, 65, 70). Therefore, we have also reexamined the tissue specificity of *Spi-1* expression by Northern (RNA) analysis and by in situ hybridization to *Spi-1* mRNA in fetal and adult mouse tissues. We have mapped the *Spi-1* oncogene locus on human chromosome 11 to a region currently devoid of identified human malignancy markers.

MATERIALS AND METHODS

Cell culture, transfection, and extracts. Both MEL (745-PC4) cells and COS-1 cells were grown in Dulbecco modified Eagle medium supplemented with 10% fetal calf serum (Armour Pharmaceutical Co.) and 2 mM L-glutamine. COS cells were transfected with DNA by electroporation. COS cells were collected by trypsinization, washed twice with cold phosphate-buffered saline (PBS), and resuspended with 0.7 ml of cold PBS per transfection sample (one T175 flask yields cells for three transfection samples). Then, 0.7 ml of cells was added to each cuvette on ice containing DNA in 100 μl of PBS, gently mixed, incubated on ice for 10 min, and electroporated with plasmid pools from a MEL cell cDNA expression library previously described (16, 83), using a Bio-Rad electroporator at 25 μF and 1,400 V. The samples were incubated on ice for 10 min before transfer of each to 10-cm-diameter dishes containing 10 ml of prewarmed medium. The transfected cells were incubated at 37°C for 48 to 72 h.

To make extracts for the expression cloning, transfected COS cells were collected by scraping and centrifugation. Cell pellets were resuspended with 25 μl of lysis buffer (1.5 mM *N*-hydroxyethylpiperazine-*N'*-2-ethanesulfonic acid [HEPES; pH 7.9], 140 mM NaCl, 1.5 mM $MgCl_2$, 0.5% Nonidet P-40, 1 mM dithiothreitol, 1 mM phenylmethylsulfonyl fluoride, 8.4 μg of aprotinin per ml, 2 μg each of antipain, leupeptin, and pepstatin per ml), transferred to an Eppendorf tube, and centrifuged in a microcentrifuge at 2,500 rpm for 10 min at 4°C. The supernatant was transferred to a new tube and either used immediately for EMSA or quick-frozen on dry ice and stored at −70°C until use. For the same extract procedure, MEL cells grown in suspension were collected by centrifugation, washed once with PBS, and resuspended with approximately 25 μl of lysis buffer per 10^6 cells.

Plasmids, DNA fragments, oligonucleotides, and end labeling. All of the double-stranded oligonucleotides described below were designed to have four-base 5′ overhangs at both ends when annealed. The sequences of the four 30-bp double-stranded oligonucleotides, O-1112, O-1516, O-1718, and O-1920, are depicted in Fig. 1A. The wild-type member of the series, O-1112, contains the mouse β^M-globin sequence from +534 to +568. The single-stranded 44-nucleotide antisense oligonucleotide, D66 (5′-TGTAACATC CAGCTGAGCTCCAGGTTGGTCAGATCCCCTGCTTC-3′), contains sequence from mostly the 5′ untranslated region of our *Spi-1*/PU.1 clone (nucleotides 14 to 56). All of

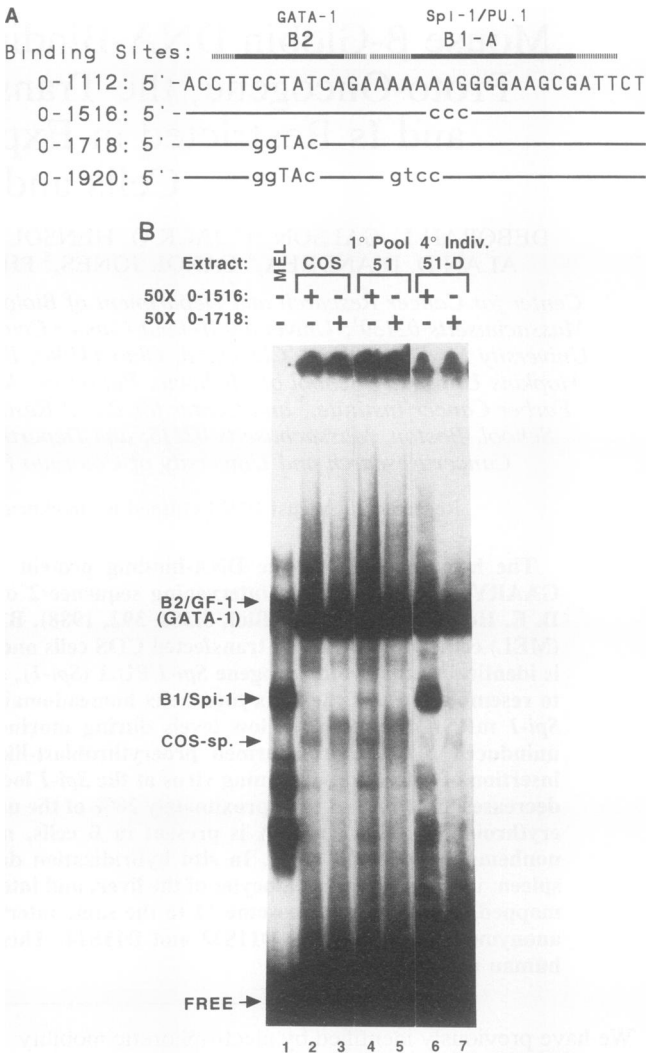

FIG. 1. Expression cloning of factor B1 cDNA. (A) Binding sites and mutations in the oligonucleotides used in the expression cloning. The filled-in sequence of the four 30-bp double-stranded oligonucleotides, O-1112, O-1516, O-1718, and O-1920, are depicted. The wild-type member of the series, O-1112, contains the mouse β-globin sequence from +535 to +568. The double-stranded oligonucleotides described above were designed to have four-base 5′ overhangs at both ends when annealed. The summation from both DNA strands of the footprints determined by methylation interference (solid bars) and DNase I protection (dashed bars) of the B2 (GATA-1) factor binding to site B2 and the B1 (*Spi-1*/PU.1) factor binding to the B1-A site are indicated (27). All of the mutations were demonstrated to abolish binding of the respective factor (data not shown). (B) Assay in which end-labeled wild-type oligonucleotide O-1112 was incubated in reaction mixtures with 5 μl of cell lysate and either 2 (lane 1) or 10 (lanes 2 to 7) μg of poly(dI-dC) · (dI-dC) in binding buffer with a final concentration of 3.5 mM $MgCl_2$ and 60 mM NaCl. All reaction mixtures contained a 50-fold molar excess of unlabeled O-1920 except lane 1 (to decrease some of the nonspecific binding by COS cells). The reaction mixtures also included a 50-fold molar excess of either unlabeled O-1516 or unlabeled O-1718 as indicated. Extracts (cell lysates) used in lanes: 1, uninduced MEL cells; 2 to 3, mock-transfected COS cells; 4 and 5, primary cDNA pool 51-transfected COS cells; 6 and 7, purified factor B1 cDNA 51-D-transfected COS cells.

the single-stranded oligonucleotides were gel purified on a preparative denaturing gel (15% polyacrylamide–8 M urea) before use as either single- or double-stranded DNAs. Plasmid GF1-pXM (83) was kindly provided by L. I. Zon.

All of the DNA probes for EMSA were end labeled by filling in 5′ overhangs with Klenow fragment and α-^{32}P-labeled deoxynucleoside triphosphates (NEN) and purified on a 10% polyacrylamide gel. DNA probes for Northern and Southern analyses were isolated from low-melting-point agarose and labeled with [α-^{32}P]dCTP, using the random-primer method of Feinberg and Vogelstein (21). The *Spi-1* probe is defined as the labeled *Xho*I-excised 1,264-bp *Spi-1* insert from clone 51-D-pXM. The oligonucleotides used for in situ RNA hybridization were labeled at the 3′ end by terminal deoxynucleotidyltransferase (Bethesda Research Laboratories) and [α-^{35}S]dATP (NEN).

EMSA. The binding reactions were carried out essentially as described by Galson and Housman (27) except that the gel system contained 0.5× TBE (1× TBE is 89 mM Tris, 89 mM boric acid, and 2.5 mM EDTA [pH 8.3]).

Sequencing. Cloned DNA was sequenced as double-stranded plasmids by the dideoxynucleotide chain termination method (74) using Sequenase (United States Biochemical). Regions of compression were resequenced with dITP and/or with 7-deaza-dGTP. The initial primers used were received from L. I. Zon and annealed to regions of the vector pXM flanking the cloning site. Additional primers in both directions were derived from the sequence as it became available. Sequence was obtained from both strands.

Ethylation interference. Single-end-labeled oligonucleotide O2-4 was ethylated (80) by incubation in 25 mM sodium cacodylate (pH 8)–50% nitrosoethylurea (Sigma)-saturated ethanol at 50°C for 45 min and then ethanol precipitated twice with 10 μg of glycogen as the carrier. Preparative EMSA and DNA elution were carried out as described previously for methylation interference assays (27). The eluted DNAs were resuspended in 20 mM sodium acetate–1 mM EDTA, cleaved by treatment with 0.19 M NaOH at 90°C for 30 min, neutralized, and ethanol precipitated twice prior to analysis on an 8% acrylamide–8 M urea sequencing gel.

RNA preparation and hybridization. RNA was isolated from MEL cells (37) and CB5 cells (79) by Triton lysis and sodium dodecyl sulfate (SDS)-phenol extraction. CEM (acute lymphocytic leukemia) and S194 (human α-secreting myeloma) RNAs were gratefully received from D. Haber and J. Parvin, respectively. RNAs were run on a 1.5% agarose gel containing 6% formaldehyde and 1× running buffer (20 mM morpholinepropanesulfonic acid [MOPS], 5 mM sodium acetate [pH 7], 1 mM EDTA) and blotted to nitrocellulose membranes (Schleicher & Schuell). The RNA blot containing total RNAs from 2D4, C57 (90), PT18 (68), BMCMC (25, 58), Pu-5, WEHI-3, NIH 3T3, Swiss 3T3, and RM4/4 cells was made and kindly given to us by M. Tsai and S. Galli (11).

Filters were prehybridized in hybridization solution (50 mM Tris [pH 7.5], 0.1% $NaPP_i$, 50% formamide [nucleic acid grade; EM Industries], 0.5% SDS, 10% dextran sulfate, 5× Denhardt's solution, 100 μg of sheared salmon sperm DNA per ml) at 42°C for 2 to 4 h. Boiled probe was added at 1×10^6 to 3×10^6 cpm/ml, and the filters were further incubated at 42°C for 16 to 48 h. Filters were washed at 60 to 65°C for 30 min each step as follows: twice in 2× SSC (1× SSC is 150 mM NaCl plus 15 mM sodium citrate)–0.1% SDS and one or two times in 1× SSC–0.1% SDS. Probe was removed from Northern blots by incubation in 50% formamide–1× SSC–1 mM EDTA at 65°C for 30 min. Damp filters were wrapped in Saran Wrap and exposed to Kodak XAR-5 film with or without a Du Pont Lightning-Plus intensifying screen.

CFU-E isolation and RNA quantitation. The CFU-E were isolated from BALB/c mouse spleens after an 84-h recovery from thiamphenicol treatment. CFU-E were purified and placed in erythroid culture as described by Boyer et al. (9). Maturing CFU-E cultures were harvested at 0, 5, 10, 20, and 46 h, and RNA was extracted from whole cells by guanidinium isothiocyanate extraction (12). RNase protection assays were used to quantitate the changing amount of β^M-globin mRNA at each time point as described by Bender et al. (6) except that 10 μM [α-^{32}P]CTP (410 Ci/mmol; Amersham) was used instead of 8 μM [α-^{32}P]UTP. Two serial dilutions of mouse reticulocyte RNA were used to (i) verify linearity in the range of mRNA concentrations used (probe excess) and (ii) quantitate the amount of β^M-globin mRNA in the samples from the different time points of CFU-E maturation. X-ray films were scanned with a densitometer (LKB), and tracings were cut out and weighed on an analytical balance. The values of the reticulocyte dilution series were plotted, and the values of β^M-globin mRNA in each sample were determined from this standard curve.

Genomic DNA analysis. Digested genomic DNAs were transferred from agarose gels to Zetabind nylon filters (AMF-Cuno) by using an alkaline transfer solution (0.4 N NaOH, 1.5 N NaCl) (52, 71) for approximately 6 h. The filters were neutralized in 2× SSC for 5 to 10 min and then pretreated for 1 h at 65°C in 0.5% SDS–0.1× SSC before first use. Filters were prehybridized at 65°C in Church's hybridization solution (0.5 M $NaHPO_4$ [pH 7.8], 7% SDS, 1% bovine serum albumin, 1 mM EDTA) (13) for 3 to 12 h, and then boiled probe was added at 1×10^6 to 3×10^6 cpm/ml. The filters were further incubated at 65°C for 18 to 48 h. Filters were washed twice each as follows: at room temperature for 5 min in 2× SSC–0.1% SDS, at 60 to 65°C for 30 min in 2× SSC–0.1% SDS, and then in 0.1× SSC–0.1% SDS. Damp filters were wrapped in Saran Wrap and exposed to Kodak XAR-5 film with or without a Du Pont Lightning-Plus intensifying screen.

In situ RNA hybridization. The mouse tissue was rapidly dissected on ice, cut at 14-μm thickness in a cryostat, and thawed onto slides pretreated with poly-L-lysine at 100 μg/ml. Protocols for hybridizations were performed essentially as described previously by Schalling et al. (75), with the modifications described by Pelletier et al. (66).

Nucleotide sequence accession number. The nucleotide sequence data reported in this paper have been submitted to GenBank and assigned accession number L03215.

RESULTS

Expression cloning of factor B1-binding activity. To clone factor B1, we used a mammalian expression system combined with EMSA analysis of extracts from transfected COS cells as the detection method. We electroporated miniprep DNAs from individual pools of 1×10^3 to 2×10^3 MEL cell cDNA clones in the expression vector pXM (16, 89) into COS cells. Electroporation of GF1-pXM, a GATA-1 cDNA in pXM isolated by Tsai et al. (83) via a similar protocol, was used as a positive control for each electroporation set. This factor, B2/GATA-1, has a binding site adjacent to B1-A (Fig. 1A) (27). To identify positive cDNA pools and to distinguish between B1 and B2 cDNAs, transfected COS lysates were assayed by EMSA for the ability to form the B1 complex with a radiolabeled wild-type oligonucleotide (O-1112) in the presence of a 50-fold molar excess of cold competitor DNA

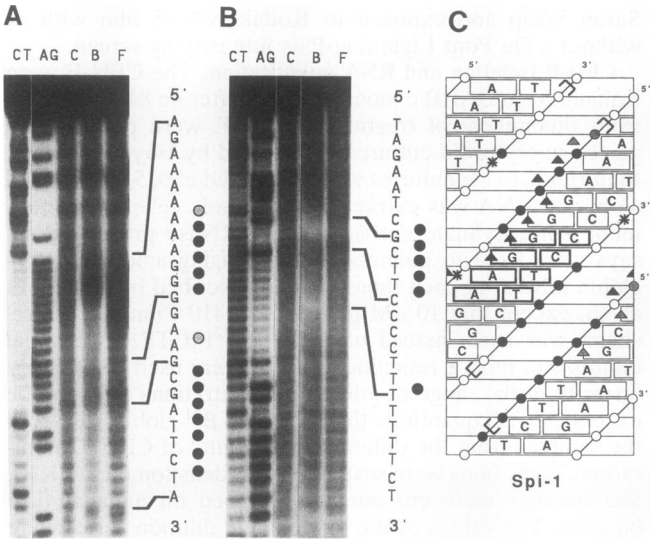

FIG. 2. *Spi-1* (B1)-DNA contacts. (A and B) Ethylation interference analysis of the *Spi-1* (B1)-DNA complex. Ethylation interference footprinting was performed as described in Materials and Methods. Oligonucleotide O2-4 (27) (containing the B1-A β^M-globin site) was labeled on the coding (A) or noncoding (B) strand. Ethylated DNAs that were not exposed to protein (lanes C) or were eluted from complex B1 (lanes B) and free DNA (lanes F) regions of a preparative EMSA gel were cleaved by alkali and analyzed by electrophoresis on a denaturing gel. Maxam and Gilbert sequencing reactions for C+T and A+G serve as markers. The sequences of both strands of the B1-A region are aligned with the gels, with the ethylated phosphates that interfered indicated by solid circles (strongly) or shaded circles (weakly). (C) Summary of the ethylation interference results from panels A and B and the DNase I protection and methylation interference results from Galson and Housman (27). The DNA is represented as a cylindrical projection. Nucleotide bases in bold boxes represent core recognition residues. Phosphates are represented as circles; phosphates which represent protein contacts are shown as solid circles (strong) or shaded circles (weak). Methylation interference positions (N-7 of guanine in the major groove and N-3 of adenine in the minor groove) are marked with solid triangles (strong) or shaded triangles (weak). *Spi-1* protected a 17-bp region on the coding strand and a 16-bp region on the noncoding strand from DNase I digestion, delimited by [and] on each strand. The asterisks mark positions of enhanced DNase I cleavage upon *Spi-1* binding.

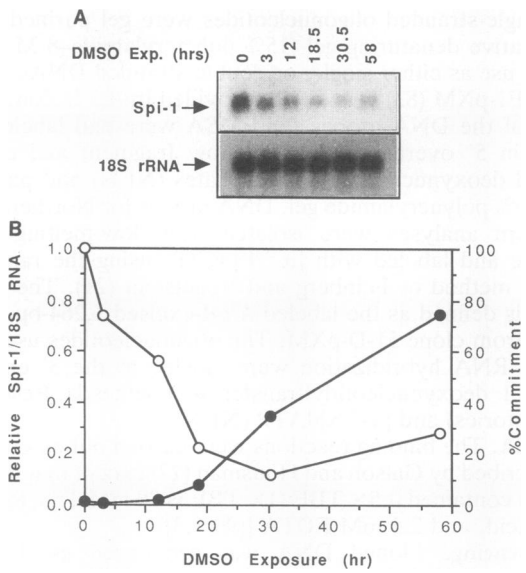

FIG. 3. Evidence that *Spi-1* decreases early in MEL cell differentiation. MEL cells were exposed to the inducer DMSO (1.5%, vol/vol), and at each of the indicated times, aliquots of cells were removed both for the commitment assay and for extraction of cytoplasmic RNA. Induction of the MEL cells by DMSO to differentiate, assessment of the percentage of cells committed to differentiation, and determination of mRNA levels were carried out as described by Hensold et al. (37). (A) Northern analysis. The labeled DNA fragments used in these experiments were the *Spi-1* probe (which detects a 1.4-kb mRNA) and a cloned fragment of the human 18S rRNA gene (87). (B) ○, both the *Spi-1* mRNA and 18S rRNA levels were quantitated by densitometry, and the *Spi-1* mRNA levels were internally standardized to the amount of 18S rRNA loaded per lane; ●, the cell aliquots removed for the commitment assay were washed and seeded at clonal density in plasma clot culture without DMSO present. After 4 days of growth, the percentage of committed cells was calculated as the percentage of the resulting colonies that reacted positively with a benzidene stain for hemoglobin.

containing either a mutated B1-A site and wild-type B2 site (O-1516) or a wild-type B1-A site and mutant B2 site (O-1718) (Fig. 1A). Of the 122 primary cDNA pools screened, three pools (e.g., pool 51) reproducibly contained a cDNA coding for a binding protein that could form a B1-like DNA-protein complex that was specifically competed for by oligonucleotide O-1718 (Fig. 1B, lane 5) and not by oligonucleotide O-1516 (Fig. 1B, lane 4). Furthermore, this complex was not present in mock-transfected COS cells (Fig. 1B, lanes 2 and 3). After three rounds of partitioning cDNA pool 51 into successively smaller pools (16, 83) and reassaying for the B1 complex by EMSA, four isolates of a single cDNA clone were obtained, an example of which is 51-D (Fig. 1B, lanes 6 and 7). Southern analysis (data not shown) of the secondary cDNA pools from the other two positive primary pools indicated that both contained an insert which cross-hybridized with 51-D.

The DNA sequence of factor B1 is identical to that of *Spi-1*/PU.1/*Sfpi-1*. The equivalence of all four of the factor B1 cDNA pool 51 isolates was demonstrated by sequencing the 5′ and 3′ ends by using flanking primers to the pXM vector. Clone 51-D cDNA was used to generate a complete sequence. The sequence of the factor B1 cDNA is essentially identical to that of the previously cloned *Spi-1*/PU.1/*Sfpi-1* (*Spi-1*) (33, 47, 55, 65) gene. *Spi-1* was isolated by both Moreau-Gachelin et al. (*Spi-1* [55, 56]) and Paul et al. (*Sfpi-1* [65]) as the gene upregulated in MEL cell lines by insertions in either orientation of the SFFV proviral genome several kilobases upstream of the transcription unit. Klemsz et al. isolated *Spi-1* as a DNA-binding protein (PU.1 [47]) that bound to the promoter of MHCII IAβ and was present in macrophage and B-cell lines. Our clone starts at bp 84 of the sequence of Klemsz et al. (47) and is exactly the same except for the location in our sequence of the poly(A) tract (9 bp long), which matches that of the isolate of Moreau-Gachelin et al. (55) and is different from that of the isolates of both Paul et al. (65) and Klemsz et al. (47). The latter contain an additional seven nucleotides (TTCTCCC) at the 3′ end and lack a reported poly(A) tract in the clone.

Mapping *Spi-1*–DNA phosphate backbone contacts. The *ets* family of transcription factors has not been associated with any specific class of DNA-binding domains because of a lack of readily identifiable primary amino acid sequence motifs (60). Since different protein DNA-binding motifs interact in distinct ways with DNA (63), an alternate approach is to

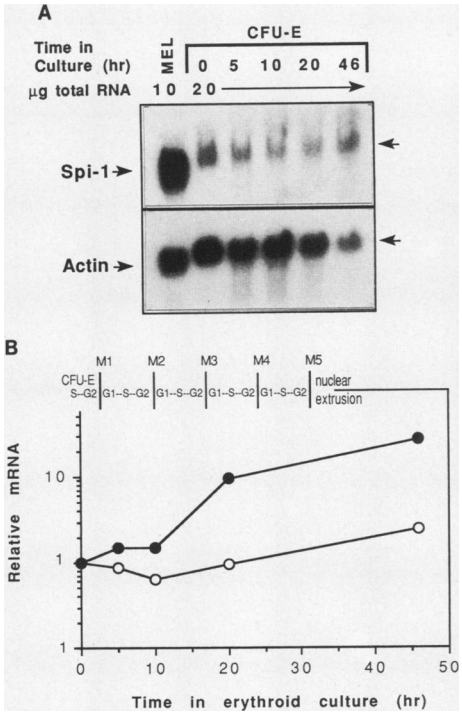

FIG. 4. Presence of *Spi-1* at low levels throughout normal CFU-E maturation. (A) Northern blot analysis. To determine the relative levels of *Spi-1* mRNA in normal CFU-E and later stages, total RNA from CFU-E maturation time point samples as indicated as well as uninduced MEL total RNA were analyzed by Northern blotting. The blot was sequentially probed with the *Spi-1* probe and a labeled cloned fragment of the chicken β-actin gene (14), using the manufacturer's protocols for GeneScreen Plus (NEN). (B) ○, *Spi-1* and actin mRNA levels were quantitated by densitometry, and the *Spi-1* results were internally standardized to the amount of actin mRNA in each lane; ●, the amount of β^M-globin mRNA at each time point was quantitated by RNase protection assays as described in Materials and Methods. The mitoses during CFU-E proliferation and maturation (51) are delineated along the top axis. By 42 h, approximately 95% of the cells had extruded their nucleus.

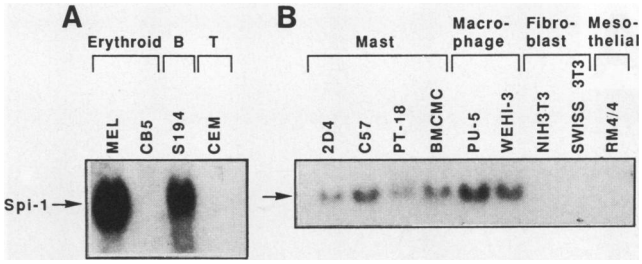

FIG. 5. RNA blot analysis of the tissue specificity of *Spi-1* expression. Northern blot analysis was performed on total RNA isolated from various cell types. (A) The RNA (10 μg) from cell lines MEL (murine CFU-E-like cell line), CB5 (murine BFU-E-like cell line), S194 (human α-secreting myeloma), and CEM (acute lymphocytic leukemia) were probed with the labeled *Spi-1* probe. The 1.4-kb *Spi-1* mRNA is indicated with an arrow. (B) RNA (10 to 15 μg) from cell types 2D4 and C57 (both IL-3-independent murine mast cell lines [90]), PT18 (IL-3-dependent long-term-cultured murine mast cells [68]), BMCMC (4-week-old primary bone marrow-derived cultured murine mast cells which represent the immature mucosal type [25, 58]), Pu-5 and WEHI-3 (both murine myelomonocytic cell lines), NIH 3T3 and Swiss 3T3 (murine fibroblast cell lines), and RM4/4 (rat peritoneal cavity-lining mesothelial cell line) were hybridized with the same probe as in panel A. The 1.4-kb *Spi-1* mRNA is indicated with an arrow.

examine the nature of the protein-DNA contacts. We have previously determined both the DNase I protection pattern and the methylated bases which interfere with *Spi-1* binding to the B1-A β^M-globin site (27) (Fig. 2C). We have now analyzed the *Spi-1*–DNA phosphate backbone contacts by ethylation interference (Fig. 2). On the coding strand (Fig. 2A), ethylation of two groups of six to seven phosphates flanking the GGAA *ets* family core motif (45) interfered with *Spi-1* binding. On the noncoding strand (Fig. 2B), a group of five phosphates overlapping most of the TTCC core and one phosphate on the other side of the core interfered with *Spi-1* binding. The positions of the most intense ethylation interference overlapped the region of strong methylation interference (Fig. 2C). Over a length of two turns, 19 of 20 backbone contacts mapped to one side of the DNA helix, whereas the DNase I-hypersensitive sites mapped to the opposite side of the helix, indicative of *Spi-1*-induced DNA helix distortion.

***Spi-1* expression during erythroid differentiation.** Previous EMSA data suggested that there might be a drop in B1 (*Spi-1*) binding during the course of DMSO-induced MEL cell differentiation (27). We therefore analyzed the expression pattern of *Spi-1* mRNA in differentiating MEL cells (Fig. 3). The amount of *Spi-1* mRNA relative to 18S rRNA drops to ~20% after 18.5 h of DMSO treatment, a time at which less than 10% of the cells have committed to differentiate. The slight rise in *Spi-1* mRNA relative to 18S rRNA at 58 h is probably not significant, as the MEL cells by this point have much less 18S rRNA per cell (84).

To determine whether *Spi-1* is normally expressed in untransformed erythroid cells, *Spi-1* mRNA expression was also examined in untransformed murine CFU-E as they matured into reticulocytes in erythroid culture (Fig. 4). Northern blot analysis using both *Spi-1* and actin probes was performed on RNA samples from a time course of CFU-E maturation (Fig. 4A), and the ratio of *Spi-1* to actin mRNA was determined (Fig. 4B). For comparison, the ratio of β-globin mRNA to total RNA was also determined as an indicator of erythroid maturation in culture (Fig. 4B). Low levels of *Spi-1* mRNA were observed throughout the maturation of normal murine CFU-E. The levels of *Spi-1* mRNA in uninduced MEL cells were at least 20-fold higher than at any of the stages of CFU-E maturation.

Cell specificity of *Spi-1* mRNA expression. To complement and extend the EMSA study of *Spi-1* (B1) tissue distribution which we previously described (27), we analyzed total RNA from a variety of cell lines (Fig. 5). The murine *Spi-1* probe efficiently cross-hybridizes with human RNA and DNA. EMSA studies had indicated that the cell line CB5 (a murine BFU-E-like cell line) did not contain detectable B1/*Spi-1*-binding activity. There was also no detectable *Spi-1* mRNA by Northern analysis (Fig. 5A). Therefore, there is even less *Spi-1* mRNA in this cell line than observed in normal murine CFU-E (Fig. 4). Northern analysis also demonstrated that *Spi-1* mRNA is present in a variety of transformed mast cell lines (both interleukin-3 [IL-3] dependent and IL-3 independent) as well as in primary cultured bone marrow-derived mast cells (which represent the normal immature mucosal type) but not in a rat mesothelial cell line (RM4/4) (Fig. 5B). As predicted (26, 27, 47), *Spi-1* mRNA was present in B-cell and macrophage cell lines but not in T-cell and fibroblast cell lines. In addition, *Spi-1* protein has been observed to be present in peripheral blood monocytes, and preliminary

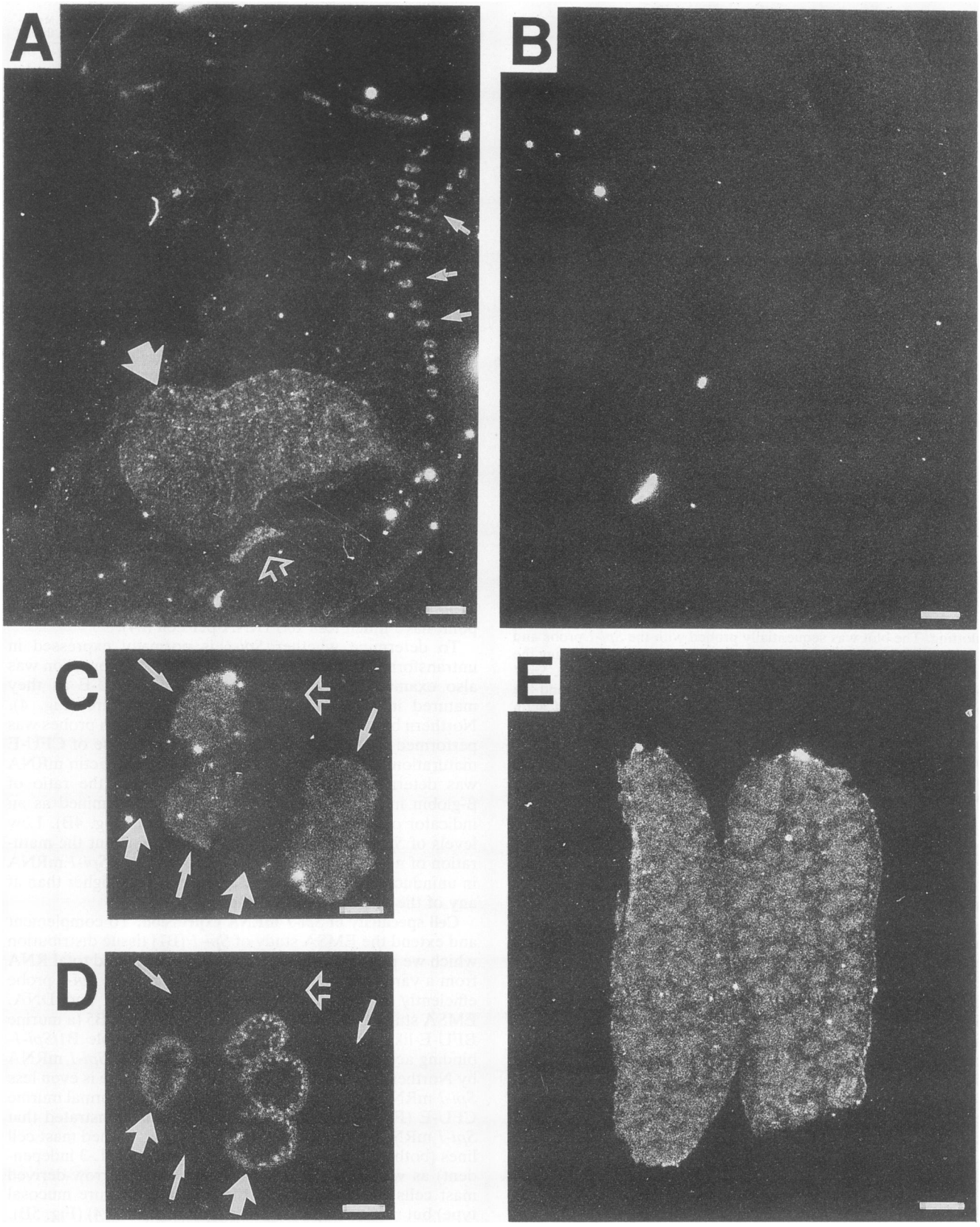

FIG. 6. In situ hybridizations to sections from a murine fetus at day 19 of gestation and adult spleen. Presented are autoradiographs after 15 days of exposure after in situ hybridization with ^{35}S-labeled oligonucleotide probes complementary to either *Spi-1* mRNA (antisense oligonucleotide D66) (A, C, and E) or WT1 mRNA (66) (B and D). *Spi-1* and WT1 mRNAs are visualized as silver grains with dark-field illumination. (A) Sagittal section of a murine fetus at day 19 of gestation. Intense labeling is apparent with the D66 probe over the liver (thick

evidence suggests that *Spi-1* mRNA is also present in elutriated rat megakaryocytes (26).

To further characterize *Spi-1* expression in normal untransformed tissues, we performed in situ RNA hybridization on fetal and adult mouse tissues by using an antisense probe from the 5′ untranslated region of the *Spi-1* gene, D66 (Fig. 6 and 7). Hybridization with an antisense probe to the murine Wilm's tumor gene (WT1) (66) rather than a *Spi-1* sense probe was performed as a control. In the whole fetus at day 19 of gestation, *Spi-1* mRNA is clearly expressed in vertebrae, liver, and spleen (Fig. 6A), a pattern not observed with the control antisense DNA probe from the WT1 gene (Fig. 6B). In a sectioned composite of isolated liver, kidneys, and adrenal glands from day 19 of gestation, *Spi-1* antisense probe D66 (Fig. 6C) hybridized to liver and not to kidney, in contrast to an antisense probe from the WT1 gene (Fig. 6D), which hybridized to kidney and not to liver. Neither probe hybridized to the adrenal gland. In addition, the maternal organs (adult) placenta and ovary were also negative for *Spi-1* expression (not shown). The pattern of hybridization to *Spi-1* mRNA in the spleen (Fig. 6E) indicates much higher expression in the nodular white pulp than in the red pulp, suggesting that the higher levels of expression observed in the B-cell, macrophage, and mast cell lines than in normal untransformed erythroid cells may reflect the normal level of expression of *Spi-1* in those cell types. Higher magnification of fetal pelvis and rib (Fig. 7A and B) demonstrate *Spi-1* expression in those bones also. The expression of *Spi-1* mRNA is limited to the marrow and does not occur in the bone-forming regions. Hybridization to a fetal liver section has a cobweb appearance that indicates that *Spi-1* expression is limited to a subset of cells and is not suggestive of hepatocyte expression (Fig. 7C). Strong hybridization was observed in fetal liver as early as day 14 of gestation (not shown). We counterstained both fetal and adult (day 17 postpartum) liver sections with hematoxylin and eosin and used a higher magnification (not shown). The pattern of in situ hybridization observed indicates again that *Spi-1* expression in liver is not due to the hepatocytes. A likely source of *Spi-1* in the liver are the Kupffer cells, which derive from the macrophage lineage. *Spi-1* expression is also detected in fetal testis in the interstitial spaces (Fig. 7D, arrows). Counterstained adult testis at a higher magnification (not shown) showed that in the testis, the seminiferous tubular Sertoli cells and germ cells do not express *Spi-1*. The hybridization to the interstitial regions of the testis is suggestive of Leydig cells but could also be due to the tissue-infiltrating mast cells and/or macrophages. However, this result correlates with the demonstration of *Spi-1* mRNA in a Leydig testicular tumor by Paul et al. (65).

Mapping of the *Spi-1* gene on human chromosome 11. The oncogenic potential of the *Spi-1* locus led us to map the position of the locus in order to gain insight into whether it may be involved in any human malignancies. In situ cytogenetic data from Nguyen et al. (59) indicated that the *Spi-1* gene locus was located on human chromosome 11, region p11.22. Therefore, we used the J1 series of human chromosome 11 somatic cell hybrids containing radiation-induced deletions and Goss-Harris hybrids to further map the location of the *Spi-1* gene (Fig. 8). The mouse *Spi-1* cDNA cross-hybridized strongly to both human and hamster DNA, and *Bgl*II digestion produced a conveniently sized restriction length polymorphism between the human (HeLa) and hamster (CHTG49) *Spi-1* genes (Fig. 8A). The parent hybrid containing all of human chromosome 11 (J1-11) was positive for the human *Spi-1* locus. The human *Spi-1* gene was also present in hybrids MJ, J1-53, J1-48, J1-9, J1-23, and J1-8 and absent in hybrids J1-7, J1-4b, J1-14, GH2, GH4, GH1, and GH3A. This result places the *Spi-1* gene in the same interval as ACP2 (lysosomal acid phosphatase) between the markers D11S33 and D11S14 (Fig. 8B), consistent with the cytogenetic results. Consequently, the *Spi-1* gene provides another locus with ACP2 to subdivide this interval. Furthermore, this is consistent with the assignment of the *Spi-1* oncogene locus to mouse chromosome 2 (55, 65), because the linkage map through this region of human chromosome 11 is highly conserved on mouse chromosome 2 (28). Although human chromosome 11 is frequently rearranged in neoplasia, no such chromosomal rearrangements have thus far been associated with the interval containing the *Spi-1* oncogene locus (42).

DISCUSSION

The *Spi-1* ETS domain contains several interesting structural motifs. We have demonstrated by cloning that the DNA-binding protein B1, which binds to two sites each within the IVS2 of both the mouse β^M- and β^m-globin genes, is identical to the proto-oncogene *Spi-1*/PU.1 (*Spi-1*), a member of the *ets* family of DNA-binding proteins (45, 47). *Spi-1* is the least related member of the *ets* family (45). Analysis of putative *Spi-1* secondary structure by both the Chou-Fasman and Garnier-Osguthorpe-Robson algorithms (18) reveals a region within the ETS domain where the results from the two algorithms correlate closely and predict the existence of three closely spaced basic α helices separated by turns (Fig. 9A). When analyzed statistically against established HTH motifs (19), and assuming a longer interhelical turn (9 amino acids), the first two *Spi-1* helices generate an SD score (19) of 2.73, indicating a reasonable probability that this is an HTH motif. Similarly, a longer turn has also been suggested for the HTH motif of the *myb* proteins (22, 24, 73). Although this HTH motif is not as convincingly represented in other *ets* proteins, the second (or DNA recognition) helix of the putative HTH domain in *Spi-1* corresponds to one of the two *ets* family signature patterns (18). It is possible that other *ets* proteins possess HTH structures which cannot be identified by analysis of primary sequence. Analysis by helical wheel projection of the putative *Spi-1* recognition helix reveals an amphipathic nature consistent with other HTH structures (10, 57). The other members of the *ets* family also contain putative am-

arrow), the spleen (open arrow), and the vertebra of the spine (small arrows). (B) Section semiadjacent to that shown in panel A hybridized with the WT1 probe. (C) Kidneys, livers, and adrenal glands dissected from murine fetuses at day 19 of gestation, mounted adjacent to each other on microscope slides and subjected to identical experimental manipulations. A cross section hybridized with probe D66 shows intense labeling over the liver (thin arrows) and none over the kidneys (thick arrows) or adrenal gland (open arrow). (D) Section adjacent to that shown in panel C hybridized with the WT1 probe, showing intense labeling over the kidneys (thick arrows) and none over the liver (thin arrows) or adrenal gland (open arrow). (E) Cross section of a spleen dissected from a day 17 postpartum (early adult) mouse hybridized with probe D66. Strong hybridization is apparent over the white pulp, and weaker hybridization is observed over the red pulp. Bars = 1 mm.

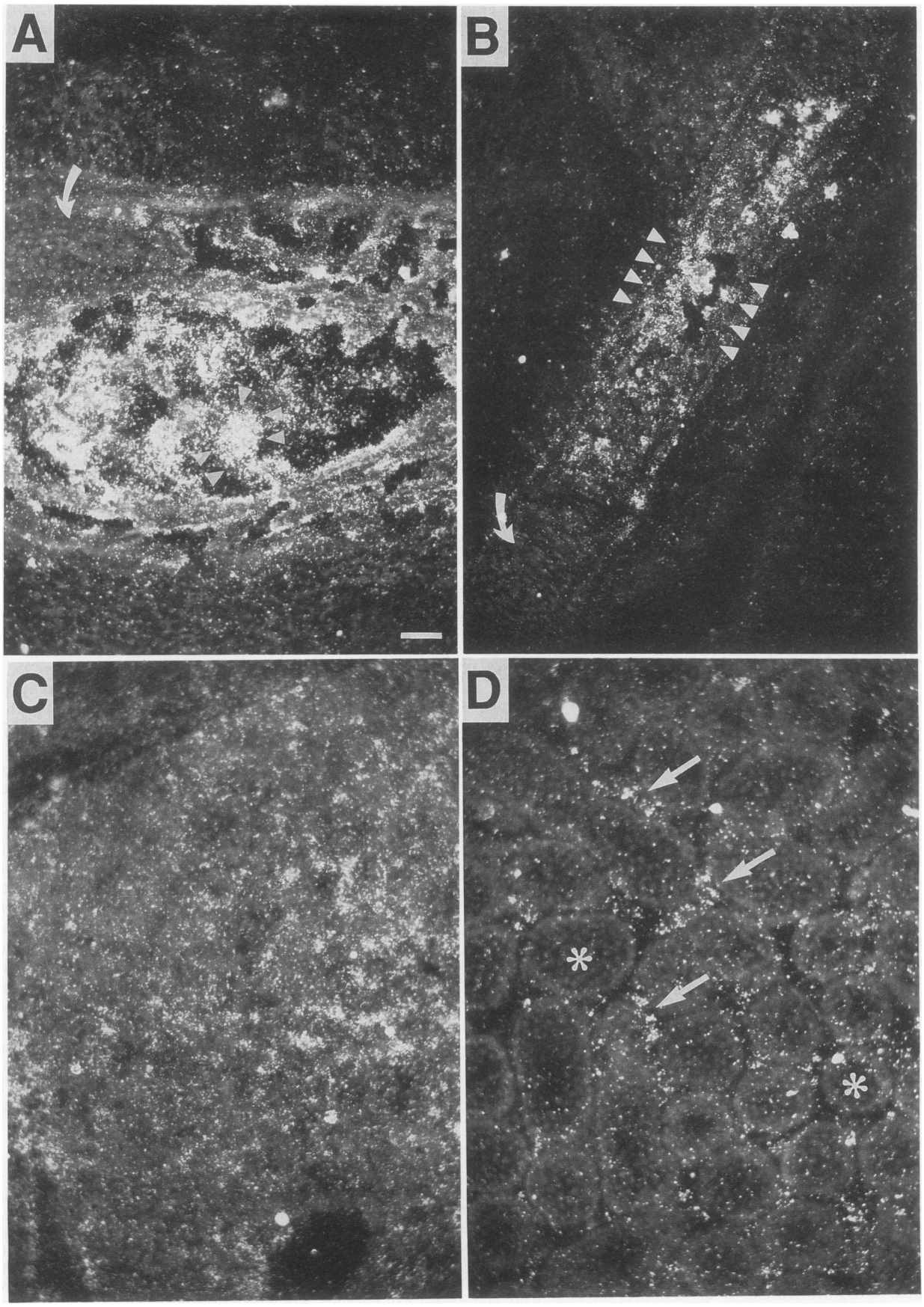
A
B
C
D

phipathic helices at homologous locations. We have observed that *Spi-1* binding at the B1-A site induces three internal bases to become hypersensitive to DNase I cleavage (27) (Fig. 2C), implying that the DNA helix becomes distorted by the interaction with *Spi-1* protein. This notion is consistent with the helix distortion induced by HTH proteins (10, 35). The DNase I-hypersensitive site between the two C's adjacent to the core motif has also been observed in an analogous location for other members of the *ets* family (60).

The putative *Spi-1* recognition helix is followed by a basic α-helical sequence located between K-244 and K-249. Deletion of these basic residues in *Spi-1* (69), in c-*ets-1* (8), and in an analogous region in *myb* (73) reduces DNA binding. Similarly, the *Drosophila* homeodomain family possesses an extended 17-amino-acid-long recognition helix containing C-terminal basic residues essential for backbone phosphate interactions (1, 46). Both *ets* and homeodomain proteins bind as monomers to a nonsymmetrical four-nucleotide-long core which is common to all family members and derive discrimination from immediately adjacent flanking nucleotides (45, 77, 86). The recent characterization of the DNA-protein interactions for several homeodomains (1, 46, 88) reveal the conserved HTH protein family-specific phosphate backbone interaction patterns. Ethylation interference analysis of phosphate backbone contacts by *Spi-1* bound to the B1-A site of β-globin (Fig. 2) and by the *ets-1* ETS domain (60) indicate a striking similarity to the conserved phosphate contacts of the HTH protein family (35, 62, 88).

At a higher structural level, we have also observed that the *Spi-1* ETS domain is divided into four contiguous repeats of 26, 26, 25, and 25 amino acids (Fig. 9B). The repeats form a consensus in which an aromatic side chain (Y or F) is sandwiched between a branched, usually aliphatic side chain (T or L) and a glutamine (Q). This triplet is surrounded by conserved charged residues. The central aromatic amino acid of the triplet (Y, F, or W) is also conserved at all four of the equivalent positions within the ETS domain consensus (45).

Sequence specificity of DNA binding by *Spi-1*. Our present results identifying factor B1-binding sites as *Spi-1* sites along with those previously identified (47, 67, 69) and a newly identified site in the human myeloid-specific CD11b gene (64) provides a basis for deriving a consensus (Fig. 10). *Spi-1* was demonstrated to have an equal affinity for the B1-A site of the mouse β^M-globin gene and the simian virus 40 Pu box (26), in contrast to a four- to fivefold-lower affinity for the κE3′ enhancer site (69). The recently identified *Spi-1* site in the CD11b gene, which was shown to be important for promoter function (64), contains AGAA (positions 6 to 9) instead of the GGAW core sequence described as essential for binding by *ets* family members (45, 60, 86), thereby indicating greater variability in this motif than had been expected. Certain mutations at positions 1 to 4 abolish *Spi-1* binding (Fig. 1A, oligonucleotides O-1516 and O-1920), whereas others do not have any effect (e.g., B1-A mutant in Fig. 10) (27), indicating the importance of these positions in the *Spi-1* recognition sequence. An oligonucleotide containing the human IL-2 gene NFIL2B region (−127 to −145) and the sequence GAAGAGGAAAAA (23) which is bound by the *ets* family member *Elf-1* (81) did not compete at 20-fold excess with the B1-A site for *Spi-1* binding (26). This site differs from the *Spi-1* consensus only at positions 1 and 11. Thus, different *ets*-related proteins share overlapping but not identical DNA-binding sequence specificity. Comparison of the *Spi-1* consensus derived here (Fig. 10) with those derived for *ets-1* and *E74A* (60) indicates that both major and minor groove contacts are important.

***Spi-1* expression.** We have demonstrated low-level expression of *Spi-1* during the maturation of CFU-E cells. Since the level of *Spi-1* does not increase as the CFU-E mature and globin transcription increases, *Spi-1* is more likely to have a role in the establishment of a permissive chromatin structure than in the induction of globin transcription. Hypersensitive sites have been strongly implicated in the establishment of a permissive chromatin conformation that is required, but not sufficient, for transcription (reviewed in reference 34). The hypersensitive site in the IVS2 of β-globin exists prior to gene transcription (2, 7, 39, 78). There is also evidence that the IVS2 of β-globin is necessary, but not sufficient, for proper gene expression (48, 49). Although the precise role of the pair of *Spi-1*-binding sites in the IVS2 of each of the murine β-globin genes has not been delineated, they are situated within the tissue-specific DNase I-hypersensitive sites and are very close to binding sites for GATA-1 and Oct-1 (27). A pair of *Spi-1*-binding sites (Pu boxes) are required for full activity in the lymphotropic papovavirus enhancer (20) and in an enhancer-minus variant of simian virus 40 (67). The presence of a tissue-specific DNase I-hypersensitive region encompassing these sites suggests that this region is important for β-globin gene regulation and that the low-level *Spi-1* expression in normal CFU-E and later stages may be an important part of this regulation. It is also possible that an *ets* family member other than *Spi-1* is responsible for the in vivo regulatory interactions at the β-globin sites.

Because of the integration of SSFV upstream of the *Spi-1* gene in MEL cells (56), the *Spi-1* mRNA level is elevated, and we have shown it to be at least 20-fold higher than in untransformed murine CFU-E (Fig. 4). As *Spi-1* has been demonstrated to bind to DNA and regulate transcription (64, 67, 69), the insertional activation of *Spi-1* may directly affect the transcription of other genes important in promoting the transformation event and blocking differentiation. Our findings that *Spi-1* mRNA decreased significantly before the cells became committed to differentiate (Fig. 3) differ from the recent report by Schuetze et al. (76) by providing quantitation and a direct correlation of the *Spi-1* mRNA decrease with the commitment process. These data raise the question of whether this early decrease in *Spi-1* mRNA level is necessary and sufficient for commitment and differentiation to occur. It is unclear whether blocking the decrease would prevent differentiation or whether interfering with *Spi-1* expression could cause the cells to differentiate without an inducing agent. Hensold et al. (36) have recently

FIG. 7. In situ hybridizations with ^{35}S-labeled antisense *Spi-1* oligonucleotide D66 to sectioned murine fetal pelvis, rib, liver, and testis from day 19 of gestation. Presented are emulsion autoradiographs after 45 days of exposure. In cross sections through a fetal pelvis (A) and fetal rib (B), intense labeling is observed in both over the marrow (between arrowheads) and not over the bone-forming regions (curved arrow). (C) Cross section through a fetal liver. The hybridization pattern is not the smooth dense pattern expected of hepatocyte expression. (D) Cross section through a fetal testis. Hybridization is observed only in the interstitial regions (arrows) and not in the cells of the seminiferous tubules (asterisk at center). Bar = 200 μm.

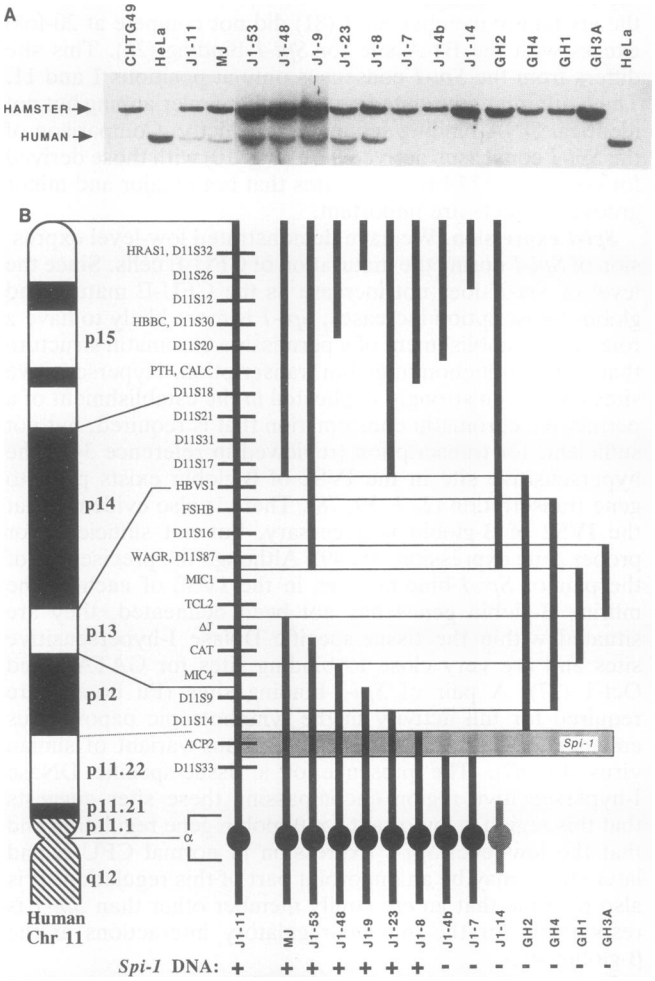

FIG. 8. Chromosomal mapping of the *Spi-1* gene locus on human chromosome 11. (A) Detection of *Spi-1* sequences by hybridization of *Bgl*II-digested genomic DNAs with the labeled *Spi-1* probe. The genomic DNAs are CHTG49 (hamster DNA), HeLa (human DNA), J1-11 (human-hamster hybrid with all of human chromosome 11), J1-4b through J1-53 (radiation-induced deletion series of human chromosome 11 derived from cell line J1-11 [41, 44]), GH-1 through GH-4 (Goss-Harris hybrids containing fragments of human chromosome 11 derived from cell line J1-11 [32]), and MJ (a somatic cell hybrid from WAGR patient MJ containing only the chromosome 11 homolog carrying an interstitial deletion limited to 11p13 [31]). The different hamster and human *Bgl*II restriction fragments detected by the *Spi-1* probe are indicated. (B) Schematic representation of the human chromosome 11p region. The segments of 11p present in the various somatic cell hybrids used for panel A are indicated by vertical solid bars in relation to an ideogram of 11p single-copy markers (28–30, 32, 41, 72). The presence (+) or absence (−) of the human *Spi-1 Bgl*II restriction fragment is indicated below each of the somatic cell hybrid 11p representations. The region within which *Spi-1* maps is indicated by a horizontal stippled zone. Genetic symbols: HRAS1, Harvey *ras* oncogene; HBBC, β-hemoglobin cluster; PTH, parathyroid hormone; CALC, calcitonin; HVBS1, hepatitus B virus insertion site; FSHB, follicle-stimulating hormone β; WAGR, WAGR complex; TCL2, T-cell leukemia breakpoint cluster region; CAT, catalase; MIC1 and MIC4, cell surface antigens defined by monoclonal antibodies; ACP2, lysosomal acid phosphatase; α, the alphoid repeat cluster which is concentrated at the centromere. All other markers are defined by anonymous DNA probes.

FIG. 9. Secondary structure predictive analysis of the ETS domain of murine *Spi-1*. (A) DNA and amino acid sequences within the ETS domain of murine *Spi-1*. The nucleotide sequence numbering starts at the beginning of our clone, and the numbering of the predicted amino acid sequence is in parentheses. The ETS domain (45) is underlined with a thick line, and the *ets* family conserved tryptophan (W) positions are circled. Note that *Spi-1*/PU.1 is missing the first of the conserved tryptophans and has a tyrosine (Y) instead. Locations of the possible helices of a putative helix-turn-helix-turn-helix motif predicted by both the Chou-Fasman and Garnier-Osguthorpe-Robson algorithms (18) are boxed with solid lines (prediction overlap) and dotted extensions (to mark the remainder of both predictions), and the region analyzed as a putative recognition helix is double underlined. (B) The four contiguous repeats within the ETS domain, aligned with the amino acid numbering to either side and a consensus written below according to Dayhoff's rules (17).

shown that the *Spi-1* transcription rate is unchanged as MEL cells differentiate and that the decrease in *Spi-1* mRNA is due to an increased rate of degradation. This effect could provide a means by which the agents inducing MEL cell differentiation could bypass the transcriptional activation of *Spi-1* by retroviral insertion.

The BFU-E-like cell line CB5 was generated by infection of newborn mice with F-MuLV (79). *Spi-1* is neither rearranged nor activated in the leukemias induced by F-MuLV (56). Instead, transformation of erythroid cells by F-MuLV frequently (75%) results in the integration of the virus upstream of the *Fli-1* (Friend leukemia integration site 1) locus, leading to the overexpression of another *ets* family member, *Fli-1* (4, 5). Similarly, the *Fli-1* locus is not rearranged in erythroleukemias transformed by the Friend complex of SFFV plus F-MuLV (4). *Spi-1* mRNA was undetectable by Northern analysis in CB5 cells (Fig. 5A); in contrast, normal CFU-E had low but detectable amounts. This lack of expression in a transformed BFU-E-like cell may represent the status of *Spi-1* expression in the untransformed BFU-E cell, suggesting that *Spi-1* expression is an indicator of and may play a role in the BFU-E-to-CFU-E transition. Alternatively, the lack of *Spi-1* expression could be a result of the transformation event or perhaps, more specifically, the overexpression of another *ets* family member, *Fli-1*.

The cell type specificity of *Spi-1* expression reported here is consistent with that previously observed by EMSA for complex B1 formation (27) and has been expanded by the examination of additional cell types. In addition to MEL lines, *Spi-1* is expressed in the human erythroid cell lines K562 and KMOE (27). Other hematopoietic cells expressing

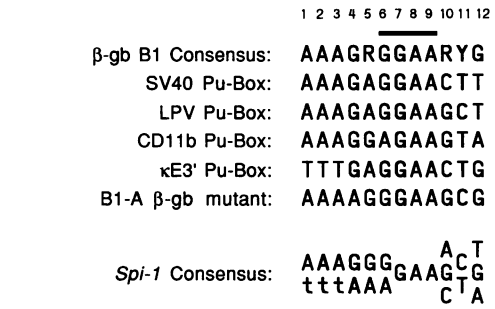

FIG. 10. Evidence that *Spi-1*-binding sites form a *Spi-1* consensus sequence. The sequences shown are described in the text. The t's in the first three positions indicates that the site containing these residues bound less well than did the others. Although positions 4 to 6 can each be an A or a G, no site has been observed to contain more than one A residue among these positions at a time. The dark line denotes the *ets* family core motif. gb, globin; SV40, simian virus 40; LPV, lymphotropic papovavirus.

Spi-1 include B cells (early pre-B through more mature stages), myelomonocytes, mast cells (both immature and mature), and possibly megakaryocytes but not T cells (Fig. 5) (27). *Spi-1* was not detected by either Northern analysis (Fig. 5) or EMSA (27) in a wide variety of nonhematopoietic cell types. By in situ hybridization, *Spi-1* was found in the hematopoietic tissues such as bone marrow, spleen, and fetal liver. In addition, *Spi-1* expression was observed in adult liver and in the testis, possibly in the Leydig cells. *Spi-1* expression was not detected in any other tissues. Therefore, in contrast to Ray et al. (70), we did not observe ubiquitous tissue expression of *Spi-1* by either RNA analysis or EMSA. Although Paul et al. (65) detected *Spi-1* expression in the heart, brain, and lung, we along with Klemsz et al. (47) did not. We also did not observe *Spi-1* expression in the fetal mouse thymus, in contrast to others who observed it in the adult mouse thymus (47, 65). It is important to note that since monocytes and mast cells contain *Spi-1* mRNA and infiltrate a variety of tissues, analysis of whole organs may give an expanded view of the tissue-specific expression profile.

The primary target genes of the *Spi-1* protein in the transformed MEL cell, as well as in the other primarily hematopoietic cell types that express this factor, have not yet been identified. Pongubala et al. (69) have recently demonstrated an enhancer function for a *Spi-1* site in the mouse immunoglobulin κ enhancer that lies downstream of the constant-region exon. In this case, *Spi-1* binding is required for another factor, NF-EM5, to bind to a distinct site. The DNA binding of other *ets* proteins has recently been reported to be enhanced by the association of unrelated proteins (15, 38, 50, 82). Overexpression of *Spi-1* may transform erythroid cells by direct binding to genes whose inappropriate expression causes the malignant transformation or by interaction with other DNA-binding proteins, thereby preventing the proper regulation of their target genes.

ACKNOWLEDGMENTS

All of the genomic DNAs for the mapping study were kindly provided by Katherine Call and David Monroe. We are very grateful to Mindy Tsai and Steve Galli for giving us the Northern blot and to Dan Haber and Jeff Parvin for RNAs. We thank David Chang and Alan Buckler for recommending the use of and methodology for the electroporation of COS cells. We also thank David Monroe, Vincent Stanton, and Hiro Aburitani for helpful advice about various protocols during the course of this work. We appreciate the contribution of Gary Quigley in discussions about the structural analysis. We extend our thanks to H. Franklin Bunn for his encouragement and support.

M.S. was supported by an EMBO fellowship. This work was supported by NIH grants P30-CA-43703 to J.O.H., DK-39888 to T.R.B., CA-18724 to C.J., AI-27850 to P.E.A., and CA-17575 to D.E.H.

REFERENCES

1. **Affolter, M., A. Percival-Smith, M. Müller, W. Leupin, and W. J. Gehring.** 1990. DNA binding properties of the purified Antennapedia homeodomain. Proc. Natl. Acad. Sci. USA **87:** 4093–4097.
2. **Balcarek, J. M., and F. A. Morris.** 1983. DNase I hypersensitive sites of globin genes of uninduced Friend erythroleukemia cells and changes during induction with dimethyl sulfoxide. J. Biol. Chem. **238:**10622–10628.
3. **Ben-David, Y., and A. Bernstein.** 1991. Friend virus-induced erythroleukemia and the multistage nature of cancer. Cell **66:**831–834.
4. **Ben-David, Y., E. B. Giddens, and A. Bernstein.** 1990. Identification and mapping of a common proviral integration site *Fli-1* in erythroleukemia cells induced by Friend murine leukemia virus. Proc. Natl. Acad. Sci. USA **87:**1332–1336.
5. **Ben-David, Y., E. B. Giddens, K. Letwin, and A. Bernstein.** 1991. Erythroleukemia induction by Friend murine leukemia virus: insertional activation of a new member of the *ets* gene family, *Fli-1*, closely linked to c-*ets-1*. Genes Dev. **5:**908–918.
6. **Bender, M. A., D. A. Miller, and R. E. Gelinas.** 1988. Expression of the human β-globin gene after retroviral transfer into murine erythroleukemia cells and human BFU-E cells. Mol. Cell. Biol. **8:**1725–1735.
7. **Benezra, R., C. R. Cantor, and R. Axel.** 1986. Nucleosomes are phased along the mouse β-major globin gene in erythroid and nonerythroid cells. Cell **44:**697–704.
8. **Boulukos, K. E., P. Pognonec, B. Rabault, A. Begue, and J. Ghysdael.** 1989. Definition of an Ets1 protein domain required for nuclear localization in cells and DNA-binding activity in vitro. Mol. Cell. Biol. **9:**5718–5721.
9. **Boyer, S. H., K. T. Landschulz, and T. R. Bishop.** 1987. Patterns of differential gene expression during maturation of erythroid colony-forming units, p. 43–54. *In* A. W. Neinhuis and G. Stamatoyannopoulos (ed.), Developmental control of globin gene expression. Alan R. Liss, New York.
10. **Branden, C., and J. Tooze.** 1991. Introduction to protein structure. Garland Publishing, Inc., New York.
11. **Burd, P. R., H. W. Rogers, J. R. Gordon, C. A. Martin, S. Jayaraman, S. D. Wilson, A. M. Dvorak, S. J. Galli, and M. E. Dorf.** 1989. Interleukin 3-dependent and -independent mast cells stimulated with IgE and antigen express multiple cytokines. J. Exp. Med. **170:**245–257.
12. **Chomczynski, P., and N. Sacchi.** 1987. Single step method of RNA isolation by acid guanidinium thiocyanate-phenol-chloroform extraction. Anal. Biochem. **162:**156–159.
13. **Church, G. M., and W. Gilbert.** 1984. Genomic sequencing. Proc. Natl. Acad. Sci. USA **81:**1991–1995.
14. **Cleveland, D. W., M. A. Lopata, R. J. MacDonald, N. J. Cowen, W. J. Rutter, and M. W. Kirschner.** 1980. Number and evolutionary conservation of α- and β-tubulin and cytoplasmic β- and γ-actin genes using specific cloned cDNA probes. Cell **20:**95–105.
15. **Dalton, S., and R. Treisman.** 1992. Characterization of SAP-1, a protein recruited by serum response factor to the c-*fos* serum response element. Cell **68:**597–612.
16. **D'Andrea, A. D., H. F. Lodish, and G. G. Wong.** 1989. Expression cloning of the murine erythropoietin receptor. Cell **57:**277–285.
17. **Dayhoff, M. O.** 1978. Atlas of protein sequence and structure, p. 345–352. National Biomedical Research Foundation, Washington, D.C.
18. **Devereux, J., P. Haeberli, and O. Smithies.** 1984. A comprehensive set of sequence analysis programs for the VAX. Nucleic

Acids Res. 12:387–395.
19. **Dodd, I. B., and J. B. Egan.** 1990. Improved detection of helix-turn-helix DNA-binding motifs in protein sequences. Nucleic Acids Res. **18**:5019–5026.
20. **Erselius, J. R., B. Jostes, A. K. Hatzopoulos, L. Mosthaf, and P. Gruss.** 1990. Cell-type-specific control elements of the lymphotropic papovavirus enhancer. J. Virol. **64**:1657–1666.
21. **Feinberg, A. P., and B. Vogelstein.** 1984. A technique for radiolabeling DNA restriction endonuclease fragments to high specific activity. Anal. Biochem. **137**:266–267. (Addendum.)
22. **Frampton, J., A. Leutz, T. J. Gibson, and T. Graf.** 1989. DNA-binding domain ancestry. Nature (London) **342**:134.
23. **Fujita, T., H. Shibuya, T. Ohashi, K. Yamanishi, and T. Taniguchi.** 1986. Regulation of human interleukin-2 gene: functional DNA sequences in the 5′ flanking region for the gene expression in activated T lymphocytes. Cell **46**:401–407.
24. **Gabrielson, O. S., A. Sentenac, and P. Fromageot.** 1991. Specific DNA binding by c-myb: evidence for a double helix-turn-helix-related motif. Science **253**:1140–1143.
25. **Galli, S. J., A. M. Dvorak, J. A. Marcum, T. Ishizaka, G. Nabel, H. der Simonian, K. Payne, J. M. Goldin, R. D. Rosenberg, H. Cantor, and H. F. Dvorak.** 1982. Mast cell clones: a model for the analysis of cellular maturation. J. Cell Biol. **95**:435–444.
26. **Galson, D. L.** Unpublished data.
27. **Galson, D. L., and D. E. Housman.** 1988. Detection of two tissue-specific DNA-binding proteins with affinity for sites in the mouse β-globin intervening sequence 2. Mol. Cell. Biol. **8**:381–392.
28. **Glaser, T.** 1988. Ph.D. thesis. Massachusetts Institute of Technology, Cambridge.
29. **Glaser, T., D. Housman, W. H. Lewis, D. Gerhard, and C. Jones.** 1989. A fine-structure deletion map of human chromosome 11p: analysis of J1 series hybrids. Somatic Cell Mol. Genet. **15**:477–501.
30. **Glaser, T., C. Jones, E. C. Douglass, and D. Housman.** 1989. Constitutional and somatic mutations of chromosome 11p in Wilm's tumor. Cancer Cells **7**:253–277.
31. **Glaser, T., W. H. Lewis, G. A. P. Bruns, P. C. Watkins, C. E. Rogler, T. B. Shows, V. E. Powers, H. F. Willard, J. M. Goguen, K. O. J. Simola, and D. E. Housman.** 1986. The β-subunit of follicle-stimulating hormone is deleted in patients with aniridia and Wilm's tumour, allowing a further definition of the WAGR locus. Nature (London) **321**:882–887.
32. **Glaser, T., E. Rose, H. Morse, D. Housman, and C. Jones.** 1990. A panel of irradiation-reduced hybrids selectively retaining human chromosome 11p13: their structure and use to purify the WAGR gene complex. Genomics **6**:48–64.
33. **Goebl, M. G., F. Moreau-Gachelin, D. Ray, P. Tombourin, A. Tavitian, M. J. Klemsz, S. R. McKercher, A. Celada, C. Van Beveren, and R. A. Maki.** 1990. The PU.1 transcription factor is the product of the putative oncogene Spi-1. Cell **61**:1165–1166.
34. **Gross, D. S., and W. T. Garrard.** 1988. Nuclease hypersensitive sites in chromatin. Annu. Rev. Biochem. **57**:159–197.
35. **Harrison, S. C., and A. K. Aggarwal.** 1990. DNA recognition by proteins with the helix-turn-helix motif. Annu. Rev. Biochem. **59**:933–969.
36. **Hensold, J. O., D. Barth, and D. L. Galson.** Submitted for publication.
37. **Hensold, J. O., G. Dubyak, and D. E. Housman.** 1991. Calcium ionophore, A23187, induces commitment to differentiation but inhibits the subsequent expression of erythroid genes in murine erythroleukemia cells. Blood **77**:1362–1370.
38. **Hipskind, R. A., V. N. Rao, C. G. F. Mueller, E. S. P. Reddy, and A. Nordheim.** 1991. Ets-related protein Elk-1 is homologous to the c-*fos* regulatory factor $p62^{TCF}$. Nature (London) **354**:531–534.
39. **Hofer, E., R. Hofer-Warbinek, and J. E. Darnell.** 1982. Globin RNA transcription: a possible termination site and demonstration of transcriptional control correlated with altered chromatin structure. Cell **29**:887–893.
40. **Johnson, P. F., and S. L. McKnight.** 1989. Eukaryotic transcriptional regulatory proteins. Annu. Rev. Biochem. **58**:799–839.
41. **Jones, C., and F. T. Kao.** 1978. Regional mapping of the gene for human lysosomal acid phosphatase (ACP2) using a hybrid clone panel containing segments of human chromosome 11. Hum. Genet. **45**:1–10.
42. **Junien, C., and O. W. McBride.** 1989. Report of the committee on the genetic constitution of chromosome 11. Cytogenet. Cell Genet. **51**:226–258.
43. **Kabat, D.** 1989. Molecular biology of Friend viral erythroleukemia. Curr. Top. Microbiol. Immunol. **148**:1–42.
44. **Kao, F. T., C. A. Jones, and C. A. Puck.** 1976. Genetics of somatic mammalian cells: genetic, immunologic, and biochemical analysis with Chinese hamster cell hybrids containing selected human chromosomes. Proc. Natl. Acad. Sci. USA **73**:193–197.
45. **Karim, F. D., L. D. Urness, C. S. Thummel, M. J. Klemsz, S. R. McKercher, A. Celada, C. Van Beveren, R. A. Maki, C. V. Gunther, J. A. Nye, and B. J. Graves.** 1990. The ETS-domain: a new DNA-binding motif that recognizes a purine-rich core DNA sequence. Genes Dev. **4**:1451–1453.
46. **Kissinger, C. R., B. Liu, E. Martin-Blanco, T. B. Kornberg, and C. O. Pabo.** 1990. Crystal structure of an engrailed homeodomain-DNA complex at 2.8 Å resolution: a framework for understanding homeodomain-DNA interactions. Cell **63**:579–590.
47. **Klemsz, M. J., S. R. McKercher, A. Celada, C. Van Beveren, and R. A. Maki.** 1990. The macrophage and B cell-specific transcription factor PU.1 is related to the *ets* oncogene. Cell **61**:113–124.
48. **Kollias, G., N. Wrighton, J. Hurst, and F. Grosveld.** 1986. Regulated expression of human $^{A}\gamma$-,β, and hybrid γβ-globin genes in transgenic mice: manipulation of the developmental expression patterns. Cell **46**:89–94.
49. **LaFlamme, S., S. Acuto, D. Markowitz, L. Vick, W. Landschult, and A. Bank.** 1987. Expression of chimeric human β- and δ-globin genes during erythroid differentiation. J. Biol. Chem. **262**:4819–4826.
50. **LaMarco, K., C. C. Thompson, B. P. Byers, E. M. Walton, and S. L. McKnight.** 1991. Identification of ets- and notch-related subunits in GA binding protein. Science **253**:789–792.
51. **Landschulz, K. T., S. H. Boyer, A. N. Noyes, O. C. Rogers, and L. P. Frelin.** 1992. Onset of erythropoietin response in murine erythroid colony-forming units: assignment to early S-phase in a specific cell generation. Blood **79**:2749–2758.
52. **Li, J. K. K., B. Parker, and T. Kowalik.** 1987. Rapid alkaline blot-transfer of viral dsRNAs. Anal. Biochem. **163**:210–218.
53. **Marks, P. A., and R. A. Rifkind.** 1978. Erythroleukemic differentiation. Annu. Rev. Biochem. **47**:419–448.
54. **Moreau-Gachelin, F., D. Ray, N. J. de Both, M. J. M. van der Feltz, P. Tambourin, and A. Tavitian.** 1990. *Spi-1* oncogene activated in Rauscher and Friend murine virus-induced acute erythroleukemias. Leukemia **4**:20–23.
55. **Moreau-Gachelin, F., D. Ray, M.-G. Mattei, P. Tambourin, and A. Tavitian.** 1989. The putative oncogene *Spi-1*: murine chromosomal localization and transcriptional activation in murine acute erythroleukemias. Oncogene **4**:1449–1456.
56. **Moreau-Gachelin, F., A. Tavitian, and P. Tambourin.** 1988. *Spi-1* is a putative oncogene in virally induced murine erythroleukaemias. Nature (London) **331**:277–280.
57. **Murre, C., P. S. McCaw, and D. Baltimore.** 1989. A new DNA binding and dimerization motif in immunoglobulin enhancer binding, *daughterless*, *MyoD*, and *myc* proteins. Cell **56**:777–783.
58. **Nabel, G., S. J. Galli, A. M. Dvorak, and H. Cantor.** 1981. Inducer T lymphocytes synthesize a factor that stimulates proliferation of cloned mast cells. Nature (London) **291**:332.
59. **Nguyen, V. C., D. Ray, M. S. Gross, M. F. de Tand, J. Frezal, and F. Moreau-Gachelin.** 1990. Localization of the human oncogene *Spi-1* on chromosome 11, region p11.22. Hum. Genet. **84**:542–546.
60. **Nye, J. A., J. M. Petersen, C. V. Gunther, M. D. Jonsen, and B. J. Graves.** 1992. Interaction of murine ETS-1 with GGA-binding sites establishes the ETS domain as a new DNA-binding motif. Genes Dev. **6**:975–990.
61. **Orkin, S. H.** 1990. Globin gene regulation and switching: circa

1990. Cell **63**:665–672.

62. **Pabo, C. O., A. K. Aggarwal, S. R. Jordan, L. J. Beamer, U. R. Obeysekare, and S. C. Harrison.** 1990. Conserved residues make similar contacts in two repressor-operator complexes. Science **247**:1210–1213.
63. **Pabo, C. O., and R. T. Sauer.** 1992. Transcription factors: structural families and principles of DNA recognition. Annu. Rev. Biochem. **61**:1053–1095.
64. **Pahl, H. L., R. J. Scheibe, H.-M. Chen, D.-E. Zhang, D. L. Galson, R. A. Maki, and D. G. Tenen.** 1993. The proto-oncogene pu.1 regulates expression of the myeloid-specific CD11b promoter. J. Biol. Chem. **268**:5014–5020.
65. **Paul, R., S. Schuetze, S. L. Kozak, C. A. Kozak, and D. Kabat.** 1991. The Sfpi-1 proviral integration site of Friend erythroleukemia encodes the *ets*-related transcription factor PU.1. J. Virol. **65**:464–467.
66. **Pelletier, J., M. Schalling, A. J. Buckler, A. Rogers, D. A. Haber, and D. Housman.** 1991. Expression of the Wilm's tumor gene WT1 in the murine urogenital system. Genes Dev. **5**:1345–1356.
67. **Pettersson, M., and W. Schaffner.** 1987. A purine-rich DNA sequence motif present in SV40 and lymphotropic papovavirus binds a lymphoid-specific factor and contributes to enhancer activity in lymphoid cells. Genes Dev. **1**:962–972.
68. **Pluznik, D. H., N. S. Tarem, M. M. Zatz, and A. L. Goldstein.** 1982. A mast/basophil cell line dependent of colony stimulating factor. Exp. Hematol. **10**(Suppl. 12):211–218.
69. **Pongubala, J. M. R., S. Nagulapalli, M. J. Klemsz, S. R. McKercher, R. A. Maki, and M. L. Atchison.** 1992. PU.1 recruits a second nuclear factor to a site important for immunoglobulin κ 3′ enhancer activity. Mol. Cell. Biol. **12**:368–378.
70. **Ray, D., S. Culine, A. Tavitian, and F. Moreau-Gachelin.** 1990. The human homologue of the putative proto-oncogene Spi-1: characterization and expression in tumors. Oncogene **5**:663–668.
71. **Reed, K. C., and D. A. Mann.** 1985. Rapid transfer of DNA from agarose gels to nylon membranes. Nucleic Acids Res. **13**:7207–7221.
72. **Rose, E. A., T. Glaser, C. Jones, C. L. Smith, W. H. Lewis, K. M. Call, M. Minden, E. Champagne, L. Bonetta, H. Yager, and D. E. Housman.** 1990. Complete physical map of the WAGR region of 11p13 localizes a candidate Wilm's tumor gene. Cell **60**:495–508.
73. **Saikumar, P., R. Murali, and E. P. Reddy.** 1990. Role of tryptophan repeats and flanking amino acids in Myb-DNA interactions. Proc. Natl. Acad. Sci. USA **87**:8452–8456.
74. **Sanger, A. F., S. Nicklen, and A. R. Coulson.** 1977. DNA sequencing with chain-terminating inhibitors. Proc. Natl. Acad. Sci. USA **74**:5463–5467.
75. **Schalling, M., K. Friberg, K. Seroogy, P. Reiderer, E. Bird, S. N. Schiffman, P. Mailleux, J.-J. Vanderhaeghen, S. Kuga, M. Goldstein, K. Kitahama, P. H. Luppi, M. Jouvet, and T. Hökfelt.** 1990. Analysis of expression of cholecystokinin in dopamine cells in the ventral mesencephalon of several species and in humans with schizophrenia. Proc. Natl. Acad. Sci. USA **87**:8247–8431.
76. **Schuetze, S., R. Paul, B. C. Gliniak, and D. Kabat.** 1992. Role of the PU.1 transcription factor in controlling differentiation of Friend erythroleukemia cells. Mol. Cell. Biol. **12**:2967–2975.
77. **Scott, M. P., J. W. Tamkun, and G. W. Hartzell.** 1989. The structure and function of the homeodomain. Biochim. Biophys. Acta **989**:25–48.
78. **Sheffrey, M., R. A. Rifkind, and P. Marks.** 1982. Murine erythroleukemia cell differentiation: DNase I hypersensitivity and DNA methylation near the globin genes. Proc. Natl. Acad. Sci. USA **79**:1180–1184.
79. **Shibuya, T., and T. W. Mak.** 1983. Isolation and induction of erythroleukemia cell lines with properties of erythroid progenitor burst-forming cell (BFU-E) and erythroid precursor cell (CFU-E). Proc. Natl. Acad. Sci. USA **80**:3721–3725.
80. **Sienbenlist, U., and W. Gilbert.** 1980. Contacts between Escherichia coli RNA polymerase and an early promoter of phage T7. Proc. Natl. Acad. Sci. USA **77**:122–126.
81. **Thompson, C. B., C.-Y. Wang, I.-C. Ho, P. R. Bohjanen, B. Petryniak, C. H. June, S. Miesfeldt, L. Zhang, G. J. Nabel, B. Karpinski, and J. M. Leiden.** 1992. *cis*-acting sequences required for inducible interleukin-2 enhancer function bind a novel Ets-related protein, Elf-1. Mol. Cell. Biol. **12**:1043–1053.
82. **Thompson, C. C., T. A. Brown, and S. L. McKnight.** 1991. Convergence of ets- and notch-related structural motifs in a heteromeric complex. Science **253**:762–768.
83. **Tsai, S.-F., D. I. K. Martin, L. I. Zon, A. D. D'Andrea, G. G. Wong, and S. H. Orkin.** 1989. Cloning of cDNA for the major DNA-binding protein of the erythroid lineage through expression in mammalian cells. Nature (London) **339**:446–451.
84. **Tsiftsoglou, A. S., W. Wong, V. Volloch, J. Gusella, and D. Housman.** 1982. Commitment of murine erythroleukemia (MEL) cells to terminal differentiation is associated with coordinated expression of globin and ribosomal genes, p. 69–79. *In* G. Akoyunoglou, A. E. Evangelopoulos, J. Georgatsos, G. Palaiologos, A. Trakatellis, and C. P. Tsiganos (ed.), FEBS meeting on cell function and differentiation. Alan R. Liss, New York.
85. **Volloch, V., and D. Housman.** 1982. Terminal differentiation of murine erythroleukemia cells: physical stabilization of end-stage cells. J. Cell Biol. **93**:390–394.
86. **Wang, C.-Y., B. Petryniak, I.-C. Ho, C. B. Thompson, and J. M. Leiden.** 1992. Evolutionarily conserved ets family members display distinct DNA binding specificities. J. Exp. Med. **175**:1391–1399.
87. **Wilson, G., B. Hollar, J. Waterson, and R. Schmeckel.** 1978. Molecular analysis of cloned 18S ribosomal DNA segments. Proc. Natl. Acad. Sci. USA **75**:5367–5371.
88. **Wolberger, C., A. K. Vershon, B. Liu, A. D. Johnson, and C. O. Pabo.** 1991. Crystal structure of a MAT α2 homeodomain-operator complex suggests a general model for homeodomain-DNA interactions. Cell **67**:517–528.
89. **Yang, Y.-C., A. B. Ciarletta, P. A. Temple, M. P. Chung, S. Kovacic, J. S. Witek-Giannotti, A. C. Leary, R. Kriz, R. E. Donohue, G. G. Wong, and S. C. Clark.** 1986. Human IL-3 (multi-CSF): identification by expression cloning of a novel hematopoietic growth factor related to murine IL-3. Cell **47**:3–10.
90. **Young, J. D.-E., C.-C. Liu, G. Butler, Z. A. Cohn, and S. J. Galli.** 1987. Identification, purification, and characterization of a mast cell-associated cytolytic factor related to tumor necrosis factor. Proc. Natl. Acad. Sci. USA **84**:9175–9179.